Clinical & Experimental Immunology
The Journal of Translational Immunology
Clinical and Experimental Immunology ORIGINAL ARTICLE doi: 10.1111/cei.13186

Heat shock proteins are differentially expressed in brain and spinal cord: implications for multiple sclerosis

R. P. Gorter,* E. Nutma,* M.-C. Jahrei,* J. C. de Jonge,† R. A. Quinlan,‡ P. van der Valk,* J. M. van Noort,§ W. Baron† and S. Amor *,¶

*Pathology Department, Amsterdam UMC, VUMC, †Department of Cell Biology, University of Groningen, University Medical Center Groningen, Groningen, ‡Department of Biosciences, Durham University, Durham, UK, §Delta Crystallon BV, Leiden, the Netherlands, and ¶Centre for Neuroscience and Trauma, Blizard Institute, Barts and the London School of Medicine and Dentistry, Queen Mary University of London, London, UK

Accepted for publication 11 July 2018
Correspondence: Professor Sandra Amor, Department of Pathology, VU University Medical Centre, 1081 HV Amsterdam, the Netherlands.
E-mail: s.amor@vumc.nl

Summary

Multiple sclerosis (MS) is a chronic neurodegenerative disease characterized by demyelination, inflammation and neurodegeneration throughout the central nervous system. Although spinal cord pathology is an important factor contributing to disease progression, few studies have examined MS lesions in the spinal cord and how they differ from brain lesions. In this study we have compared brain and spinal cord white (WM) and grey (GM) matter from MS and control tissues, focusing on small heat shock proteins (HSPB) and HSP16.2. Western blotting was used to examine protein levels of HSPB1, HSPB5, HSPB6, HSPB8 and HSP16.2 in brain and spinal cord from MS and age-matched non-neurological controls. Immunohistochemistry was used to examine expression of the HSPs in MS spinal cord lesions and controls. Expression levels were quantified using ImageJ. Western blotting revealed significantly higher levels of HSPB1, HSPB6 and HSPB8 in MS and control spinal cord compared to brain tissues. No differences in HSPB5 and HSP16.2 protein levels were observed, although HSPB5 protein levels were higher in brain WM *versus* GM. In MS spinal cord lesions, increased HSPB1 and HSPB5 expression was observed in astrocytes, and increased neuronal expression of HSP16.2 was observed in normal-appearing GM and type 1 GM lesions. The high constitutive expression of several HSPBs in spinal cord and increased expression of HSPBs and HSP16.2 in MS illustrate differences between brain and spinal cord in health and upon demyelination. Regional differences in HSP expression may reflect differences in astrocyte cytoskeleton composition and influence inflammation, possibly affecting the effectiveness of pharmacological agents.

Keywords: alpha-B crystallin, HSP16.2, HSPBs, HSPB1, HSPB5, HSPB6, HSPB8, HSPB11, multiple sclerosis, pathology, spinal cord

Introduction

Multiple sclerosis (MS) is a demyelinating disease of the central nervous system (CNS), characterized by the development of focal inflammatory lesions in the brain, optic nerve and spinal cord [1]. Previous investigations into regional heterogeneity have highlighted differences in microglia [2] and astrocyte [3] origins, morphology and function as well as blood–brain barrier permeability [4] and inflammation [5] within the CNS. The high local diversity suggests that well-studied disease mechanisms in MS-affected brains may not be directly translatable to other areas of the CNS. For example, treatment of traumatic injury with cyclosporin A reduces cortical damage in the brain [6], but not the spinal cord of rats [7], demonstrating that CNS areas react differently to pharmacological agents. Using magnetic resonance imaging (MRI), the spinal cord has been shown to be affected in approximately 85% of MS patients by lesion development and/or generalized atrophy [8]. Spinal cord lesions influence functional connectivity as visualized by MRI [9], probably contributing to the development of lower body symptoms, such as walking difficulties, bladder problems

and erectile dysfunction, which severely impact upon quality of life in people with MS [10,11]. Conversely, while spinal cord involvement in MS has high clinical relevance, few studies have investigated spinal cord lesions and fewer studies have compared spinal cord and brain pathology directly.

The comparative pathology studies demonstrate that, similar to the brain, MS spinal cord is affected by focal demyelination in white and grey matter, microglial proliferation, macrophage and T cell infiltration, astrogliosis, axon degeneration and neuronal loss [11–16]. In MS spinal cord, the extent of white as well as grey matter demyelination is high compared to brain regions [17]. Relative to the brain, the spinal cord in MS contains few (chronic) active inflammatory lesions, but relatively more inactive and remyelinated lesions, suggesting that spinal cord MS pathology is less severe than the brain [11,18,19]. However, unlike in the brain, incomplete remyelination in the spinal cord correlates with clinical disability [11]. Additionally, *in-vitro* studies examining traumatic spinal cord injury have shown that similar mechanical insults elicit a significantly stronger inflammatory reaction in the spinal cord compared to the brain, characterized by more extensive lymphocyte recruitment, microglia and macrophage activation, astrogliosis and blood–spinal cord barrier breakdown [20,21].

In response to stressors such as inflammation and oxygen radicals, cells up-regulate their basal expression of heat shock proteins (HSPs) to promote survival by preventing protein aggregation and by promoting degradation of improperly folded proteins [22]. HSPs can be classified into several families, including the small heat shock proteins (HSPB1-10), which serve crucial functions in neuroinflammation through their actions as molecular chaperones, cytoskeleton stabilizers and signalling molecules [23]. Compared to normal-appearing white matter (NAWM), expression of a number of HSPBs is increased in oligodendrocytes and reactive astrocytes in brain white matter (WM) lesions [24,25], but although cell populations and tissue responses are markedly different in the spinal cord, it was previously unclear whether spinal cord cells differentially express HSPBs during MS lesion formation.

In this study, we compared expression levels of HSPB1, HSPB5, HSPB6, HSPB8 and the orphan small heat shock protein HSP16.2 in WM and grey matter (GM) of spinal cord and brain and evaluated expression of these HSPs during MS lesion development. We show that in spinal cord MS lesions, HSPBs are predominantly up-regulated in astrocytes, similar to the brain, but that expression levels of several HSPBs is markedly higher in the spinal cord and subtly different during lesion formation.

Materials and methods

Spinal cord tissue

Spinal cord of 24 MS cases and 13 non-neurological controls (Table 1) was collected post-mortem in the pathology department of the VU Medical Centre (VUMC), the Netherlands, with the approval of the VUMC Medical Ethical Committee Samples according to the protocol of the Netherlands Brain Bank (coordinator Dr I. Huitinga, Amsterdam, the Netherlands). Tissues were fresh-frozen or fixed in formalin and embedded in paraffin. Participants had given informed consent for autopsy and use of materials for research.

Western blotting

GM and WM from eight age-matched non-neurological controls [mean age = 71·5 years (62·3–80·7)] and eight MS patients [mean age = 71·5 years (63·3–79·7)] was obtained from fresh-frozen blocks containing control white matter (CWM) and/or control grey matter (CGM) or NAWM and/or normal-appearing grey matter (NAGM). For spinal cord, GM and WM were separated manually. Samples were homogenized in TNE buffer [50 mM Tris-HCl, 150 mM M NaCl and 5 mM ethylenediamine tetraacetic acid (EDTA), pH 7·5]. Total protein concentration was measured using Bio-Rad DC Protein Assay (Bio-Rad Laboratories, Hercules, CA, USA) with bovine serum albumin (BSA) as standard. Equal amounts of protein (50 μg) and sodium dodecyl sulphate (SDS) reducing loading buffer were mixed and samples were denatured at 95°C for 5 min. Proteins were separated by 15% SDS-polyacrylamide gel electrophoresis (PAGE) and transferred to immobilon-FL transfer membrane (Merck Millipore, Burlington, MA, USA) using a semidry blotting system. After three washes with phosphate-buffered saline (PBS), membranes were blocked in Odyssey blocking buffer for 1 h (1 : 1 with PBS; Li-Cor Biosciences, Lincoln, NE, USA), followed by incubation with primary antibodies (Table 2) overnight at 4°C. After washing with PBS containing 0·05% Tween-20, membranes were incubated with the appropriate IRDye®-conjugated secondary antibodies (1 : 3000; Li-Cor Biosciences). Membranes were scanned with Odyssey version 3.0 analysis software. Subsequently, Scion Image software was used to analyse intensity. Actin was used as a loading control.

Statistical analysis

To compare HSPB expression in MS and controls, WM and GM and brain and spinal cord, values from each blot were normalized to a reference sample. Data were tested for normality and equality of variances using

Table 1. Patient characteristics

Case	Gender	Age (years)	DD (years)	MS type	PMD (h:m)	Cause of death	Tissue
Fresh-frozen tissue							
MS patients							
1	M	63	24	PP	7:05	Cardiac arrest; ruptured abdominal aorta aneurysm	B, T
2	M	71	25	PP/SP	7:00	Pneumonia by aspiration	B, T
3	M	56	14	PP	9:50	Cachexia; exhaustion; terminal phase MS	B, T
4	M	83	21	PP	7:50	Aspiration pneumonia; lung cancer	B, T
5	F	66	16	SP	10:45	Pulmonary hypertension	B, T
6	F	81	27	SP	4:35	Aspiration pneumonia	B, T
7	M	70	47	PP	6:55	Acute heart failure; *Clostridium difficile* colitis	B, T
8	F	82	60	SP	8:35	Euthanasia	B, T
Controls							
1	M	71	n.a.	CON	7:40	Sepsis	B, T
2	F	61	n.a.	CON	6:50	Euthanasia	B, L
3	M	62	n.a.	CON	7:20	Unknown	B, unkn.
4	F	78	n.a.	CON	7:10	Euthanasia	B, T
5	F	60	n.a.	CON	8:10	Metastasized mammary carcinoma	B, L
6	M	93	n.a.	CON	7:40	Heart failure	B, T
7	F	72	n.a.	CON	6:50	Euthanasia; metastasized ovarian cancer; ileus	B, L
8	F	75	n.a.	CON	9:10	Euthanasia	B, T
Paraffin-embedded tissue							
MS patients							
2	M	71	25	PP/SP	7:00	Pneumonia by aspiration	T
5	F	66	16	SP	10:45	Pulmonary hypertension	T
6	F	81	27	SP	4:35	Aspiration pneumonia	C, L
9	M	64	34	SP	7:30	Terminal phase MS; spastic MS	T
10	F	84	34	PP	<0:01	Euthanasia	unkn.
11	F	44	5	PP	10:15	Decompensation	T
12	M	56	21	SP	8:00	Pneumonia	T
13	F	69	53	PP/SP	7:30	Respiratory failure; heart failure	T
14	M	47	6	PP/SP	7:15	Urosepsis; organ failure	T
15	M	61	18	SP	9:15	Euthanasia	T
16	F	77	24	PP	10:00	Euthanasia	T
17	F	67	25	SP	9:15	Palliative sedation; shortness of breath	T
18	M	44	21	PP	10:15	Possible infection due to terminal phase MS	T
19	F	76	25	SP	7:55	Euthanasia; lung cancer with brain metastases	T
20	M	54	12	PP	8:15	Euthanasia	T
21	F	50	17	SP	7:35	Euthanasia	T
22	F	54	31	PP/SP	9:20	Heart failure	T
23	M	58	18	SP	9:15	Pneumonia; terminal renal insufficiency	T
24	M	63	25	SP	8:15	Pneumonia; cachexia; dehydration	C
Controls							
2	F	61	n.a.	CON	6:50	Euthanasia	unkn.
9	M	67	n.a.	CON	4:30	Cardiac shock; multiple organ failure	unkn.
10	M	81	n.a.	CON	5:30	Metastasized prostate carcinoma	unkn.
11	F	91	n.a.	CON	7:45	Decompensatio cordis	unkn.
12	M	67	n.a.	CON	18:35	Myocardial infarction	C
13	F	84	n.a.	CON	4:45	Respiratory failure	T

PM = post mortem; M = male; F = female; CON = control; MS = multiple sclerosis; SP = secondary progressive; PP = primary progressive; n.a. = not applicable; m = months; B = brain; C = cervical; T = thoracic; L = lumbar; S = sacral; unkn. = unknown.

Bartlett's test and the Brown–Forsythe test. Accordingly, analysis of variance (ANOVA) or Kruskal–Wallis test was performed. When significant differences were found, Sidak's or Dunn's multiple comparisons test were used for *post-hoc* testing. When HSP levels showed high individual variability, data were expressed as relative values (brain WM = 1) to compare differences in HSPB expression between WM and GM as well as spinal cord and brain. Data were tested for normality using the Kolmogorov–Smirnov normality test. To compare expression to brain WM, one-sample *t*-test or Wilcoxon's signed-rank test was used. To compare between other groups,

Table 2. Antibodies

Antigen	Antibody number	Species	Clone	Dilution IHC/WB	Incubation time	Company
(a) Primary antibodies						
HSPB1	AB155987	Rabbit	Monoclonal	1:1500/1:1000	O/N	Abcam
HSPB5	JAM01	Mouse	Monoclonal	1:750/1:200	O/N	In house
HSPB6	AB184161	Rabbit	Monoclonal	1:50000/1:2000	O/N	Abcam
HSPB8	AB96837	Rabbit	Polyclonal	1:3500/1:2000	O/N	Abcam
HSP16.2	NBP1-88332	Rabbit	Polyclonal	1:50	O/N	Novus
HLA-DR	14-99-56-82	Mouse	Monoclonal	1:1000	1 h	eBioscience
olig2	AB9610	Rabbit	Polyclonal	1:750	O/N	Millipore
Vimentin	V9	Rabbit	Mouse	1:128000	1 h	In house
(b) Secondary antibodies						
EnVision HRP anti-rabbit		Goat		Undiluted		Dako
EnVision HRP anti-mouse		Goat		Undiluted		Dako
Goat anti-mouse AP		Goat		1:250		Dako
Goat anti-rabbit AP		Goat		1:250		Southern Biotech

olig2 = oligodendrocyte transcription factor 2; HSPB = small heat shock protein; HLA-DR = human leucocyte antigen D-related; HRP = horseradish peroxidase; AP = alkaline phosphatase, O/N = overnight; IHC = immunohistochemistry.

two-sided unpaired Student's *t*-test or Mann–Whitney *U*-test was performed. Results were considered statistically significant when $P < 0{\cdot}05$.

Immunohistochemistry

Serial 5-μm paraffin sections were cut of spinal cord tissue from six non-neurological controls [mean age = 75·2 years (62·8–87·6)] and 19 MS patients [mean age = 62·4 years (56·6–68·3)]. Sections were taken from CWM (n = 6), NAWM (n = 5), active lesions (n = 4–5), chronic active lesions (n = 4–5), inactive lesions (n = 4), CGM (n = 4-5), NAGM (n = 4-5), GM type I lesions (n = 8) and GM type II lesions (n = 4). All sections were stained for proteolipid protein (PLP), human leucocyte antigen receptor D-related (HLA-DR) and double-stained for HSPB1, HSPB5, HSPB6, HSPB8, HSP16.2 and HLA-DR, olig2 and vimentin. Sections were deparaffinized with xylene, rehydrated in graded ethanol solutions and washed in water. Endogenous peroxidase was blocked by incubating the slides in PBS containing 0.3% (v/v) hydrogen peroxide for 30 min. After washing in PBS, heat-mediated antigen retrieval was performed using either 0·01 M citrate buffer (pH 6) or EDTA buffer (pH 9). After cooling and washing in PBS, slides were incubated for 1 h or overnight with primary antibodies (Table 2) diluted in normal antibody diluent (Immunologic, Duiven, the Netherlands) at room temperature (RT). Sections were washed and incubated with the secondary antibody: goat anti-mouse horseradish peroxidase (HRP) Envision (Dako, Carpenteria, CA, USA) for HSPB5 and goat anti-rabbit HRP Envision (Dako) for other HSPBs. After washing with PBS, the staining was developed with 3,3′-diaminobenzidine (DAB; Dako) at a 1 : 50 concentration for 10 min. For single staining (PLP and HLA-DR), slides were washed in tap water and nuclei were counterstained with haematoxylin, dehydrated in ascending alcohol concentrations and xylene and mounted with Quick-D (Klinipath, Duiven, the Netherlands).

To identify HSPB expression in MS lesions, double-labelling was performed for HSPBs and HLA-DR (microglia). To identify other cells expressing HSPBs, double-labelling was performed for olig2 (oligodendrocytes) or vimentin (astrocytes). Sections were stained with HSPBs as described above, and after developing with DAB the slides were washed and incubated with the second primary antibody for 1 h or overnight (Table 2). When primary antibodies were from the same species, the antibody directed to the first antigen of choice was detached by heating in citrate buffer for 15 min. After washing, the appropriate secondary antibody, goat anti-mouse alkaline phosphatase (AP) or goat anti-rabbit AP, was applied for 1 h. After washing twice with PBS and once with Tris-buffered saline (TBS), slides were developed with liquid permanent red (LPR; Dako; 1 : 100) for 10 min. Slides were washed in tap water and nuclei were counterstained with haematoxylin, washed with tap water and mounted with aquatex (Merck, Darmstadt, Germany). Following omission of primary antibodies, no staining was observed.

Digital quantification

HSPB expression was analysed using ImageJ to determine the DAB^+ pixels. For each region of interest, four to five pictures of HSPB/HLA-DR double-staining were taken at ×400 magnification using an Olympus BX41 microscope equipped with a Leica MC170 HD camera. Thresholds were set to eliminate background expression. Next, using

the macro supplied in Supporting information, Appendix A, brown DAB staining was separated from blue haematoxylin staining and pink LPR staining and the DAB$^+$ area fraction was determined.

Statistical analysis

Using GraphPad Prism version 6 (GraphPad Software, La Jolla, CA USA;_https://www.graphpad.com/scientific-software/prism/), differences in HSPB expression in WM and GM lesions were examined. Data was tested for normality. Then, expression in CWM/CGM and NAWM/NAGM was compared using Student's *t*-test or Mann–Whitney *U*-test. When expression in NAWM/NAGM did not differ from controls, other groups were compared to NAWM/NAGM. When expression differed, other groups were compared to controls. ANOVA and Dunnett's *post-hoc* testing or Kruskal–Wallis H-test and Dunn's *post-hoc* testing was performed ($P < 0{\cdot}05$).

Results

Increased HSPB1, 6, 8 protein levels in spinal cord compared to brain

Western blotting was used to compare protein levels of HSPB1, HSPB5, HSPB6, HSPB8 and HSP16.2 in fresh-frozen brain and spinal cord blocks from MS cases and non-neurological controls (Table 1). Blocks were screened by immunostaining sections for PLP and HLA-DR to select regions containing CWM/CGM in controls and NAWM/NAGM in MS cases to exclude blocks containing lesions. Although increased mRNA levels of HSPB1, HSPB6 and HSPB8 have been reported previously in MS brain NAWM [24], no differences in HSPB or HSP16.2 protein expression were found between controls and MS patients (Supporting information, Fig. 1). However, a marked increase in HSPB1 (Fig. 1a–c; $P = 0{\cdot}0078$; $P = 0{\cdot}0409$), HSPB6 (Fig. 1d–f; $P = 0{\cdot}0111$; $P = 0{\cdot}0078$) and HSPB8 (Fig. 1g–i; $P = 0{\cdot}0286$; $P = 0{\cdot}0016$) protein levels was observed in the WM of spinal cord tissues compared to brain WM in controls and MS patients, respectively. Similarly, in spinal cord GM, HSPB1 (Fig. 1a–c; $P = 0{\cdot}0070$; $P = 0{\cdot}0003$) and HSPB6 (Fig. 1d–f; $P = 0{\cdot}0104$; $P = 0{\cdot}0002$) levels were significantly higher than in brain GM, in controls as well as MS patients, but no differences were found for HSPB8 (Fig. 1g–i; $P = 0{\cdot}1506$; $P = 0{\cdot}2368$). Contrastingly, HSPB5 (Fig. 1j–l) and HSP16.2 (Fig. 1m–o) expression did not differ between spinal cord and brain samples in MS patients or controls, but the variance in the expression levels, particularly of HSPB5, was noticeably greater for MS patients. HSPB5 expression was also significantly higher in brain WM compared to brain GM in controls (Fig. 1k; $P = 0{\cdot}0078$), but not in MS patients (Fig. 1l; $P = 0{\cdot}1953$). For HSP16.2, bands were not only observed at 16 kDa, which is the predicted molecular weight, but also approximately 40, 60, 70 and 250 kDa, possibly indicating the presence of HSP16.2 complexes (Supporting information, Fig. 2). Of note, these bands were present in the brain, especially in the GM, but not in the spinal cord.

Spinal cord lesions are classified based on inflammatory activity or location

Next, we evaluated expression of HSPB1, HSPB5, HSPB6, HSPB8 and HSP16.2 in CWM, CGM, NAWM, NAGM and upon lesion development in the spinal cord. WM lesions were classified as active, chronic active or inactive based on PLP staining and HLA-DR expression (Fig. 2). Active lesions (Fig. 2a,b) and the rim of chronic active lesions (Fig. 2c,d) were characterized by extensive microglial activation and macrophage infiltration, while inactive lesions (Fig. 2e,f) were devoid of HLA-DR$^+$ cells. As GM lesions feature little microglial activity, brain GM lesions are classified in type I to IV based on their location. The spinal cord differs in anatomical structure, thus we limited classification of spinal cord lesions to type I (mixed WM and GM lesions; Fig. 2g,h) and type II (pure GM lesions; Fig. 2I,j).

Astrocytes up-regulate HSPB1 in MS spinal cord lesions

Consistent with protein analysis (Fig. 1a,c), HSPB1 was expressed constitutively in CWM (Fig. 3a) and NAWM (Fig. 3b) in the cytoplasm of cells with an astrocyte-like morphology. In MS lesions, HSPB1 expression was observed in cells with an astrocyte morphology (Fig 3c–g). Such expression was increased significantly in the rim of chronic active lesions (Fig. 3; $P = 0{\cdot}0474$) and in inactive lesions (Fig. 3f,g; $P = 0{\cdot}0369$) in vimentin$^+$ astrocytes (insert Fig. 3). In the centre of chronic active lesions, a trend towards increased HSPB1 expression was seen (Fig. 3e,g; $P = 0{\cdot}0895$). In CGM (Fig. 3i) and NAGM (Fig. 3j), HSPB1 expression was observed sparsely in the soma and axons of neurones and occasionally in astrocytes (insert in k), but was not changed significantly in GM lesions (Fig. 3h,k,l).

HSPB5 expression is increased in active lesions and the rim of chronic active lesions

In CWM (Fig. 4a), sparse HSPB5 expression was observed in cells with an astrocyte-like morphology and in oligodendrocyte (progenitor cells), as confirmed with oligodendrocyte lineage marker Olig2 (insert Fig. 4a). In comparison, a slight, but statistically significant, increase

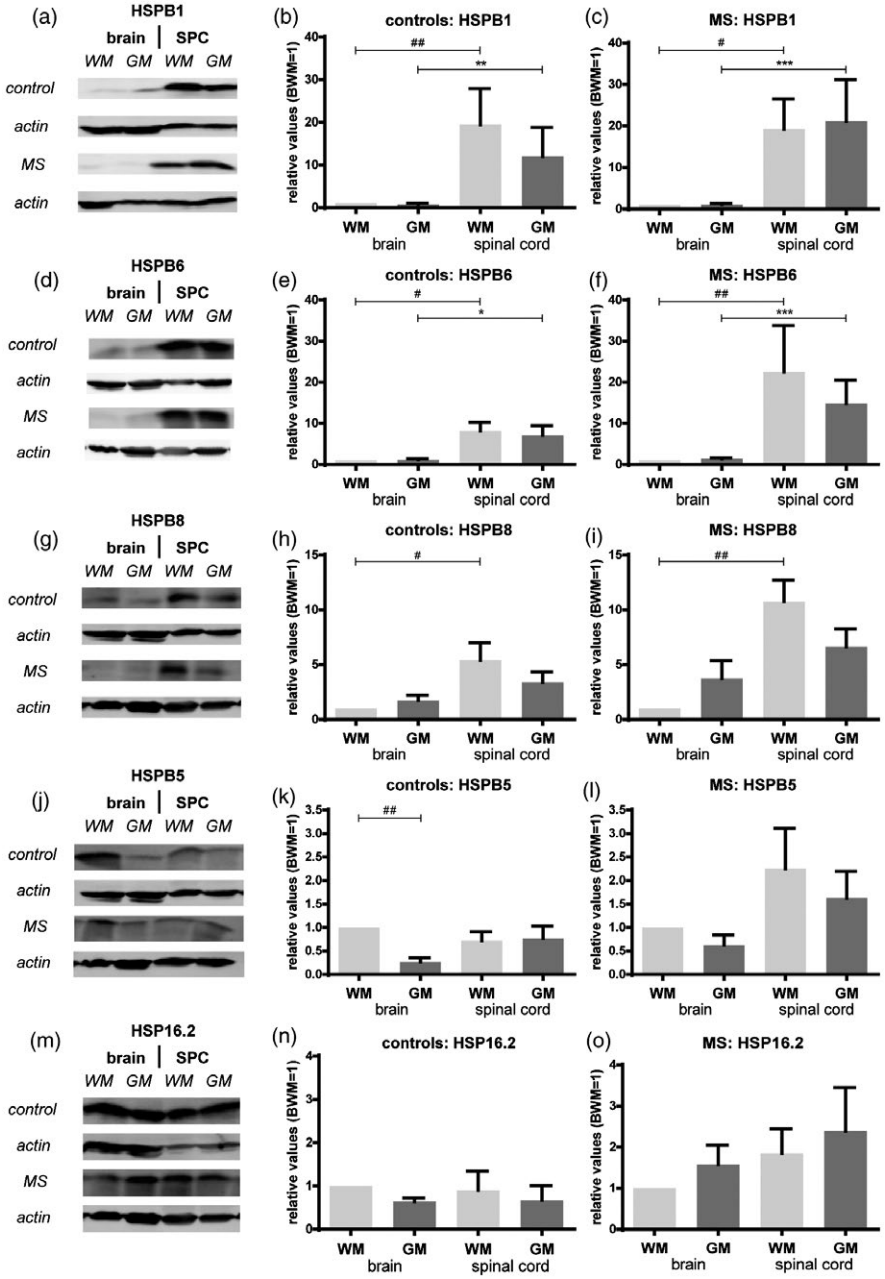

Fig. 1. Heat shock protein (HSP) levels in brain and spinal cord. Heat shock protein B (HSPB) 1, HSPB5, HSPB6, heat shock protein B (HSPB)8 and HSP16.2 protein levels in brain white matter/grey matter (WM/GM) and spinal cord WM/GM of controls ($n = 8$) and multiple sclerosis (MS) patients ($n = 8$) were determined using Western blotting and quantified with Scion Image. Representative blots are shown (top to bottom: HSP controls, actin controls, HSP MS patients, actin MS patients). Actin was used as a loading control. Values are expressed as ratio of brain WM (BWM = 1). (a) Western blot featuring HSPB1 protein levels. (b) Quantification HSPB1 protein levels controls. (c) Quantification HSPB1 protein levels MS patients. (D) Western blot featuring HSPB6 protein levels. (e) Quantification HSPB6 protein levels controls. (f) Quantification HSPB6 protein levels MS patients. (g) Western blot featuring HSPB8 protein levels. (h) Quantification HSPB8 protein levels controls. (i) Quantification HSPB8 protein levels MS patients. (j) Western blot featuring HSPB5 protein levels. (k) Quantification HSPB5 protein levels controls. (l) Quantification HSPB5 protein levels MS patients. (m) Western blot featuring HSP16.2 protein levels. (n) Quantification HSP16.2 protein levels controls. (o) Quantification HSP16.2 protein levels MS patients. To compare expression in brain and spinal cord WM, one-sample *t*-test or Wilcoxon's signed rank test was used. Significant data are presented ($^{\#\#\#\#}P < 0{\cdot}0001$, $^{\#\#\#}P < 0{\cdot}001$, $^{\#\#}P < 0{\cdot}01$, $^{\#}P < 0{\cdot}05$). To compare expression between other groups, unpaired Student's *t*-test or Mann–Whitney *U*-test was performed. Data are presented as mean with standard error of the mean. Significant data are presented ($^{****}P < 0{\cdot}0001$, $^{***}P < 0{\cdot}001$, $^{**}P < 0{\cdot}01$, $^{*}P < 0{\cdot}05$).

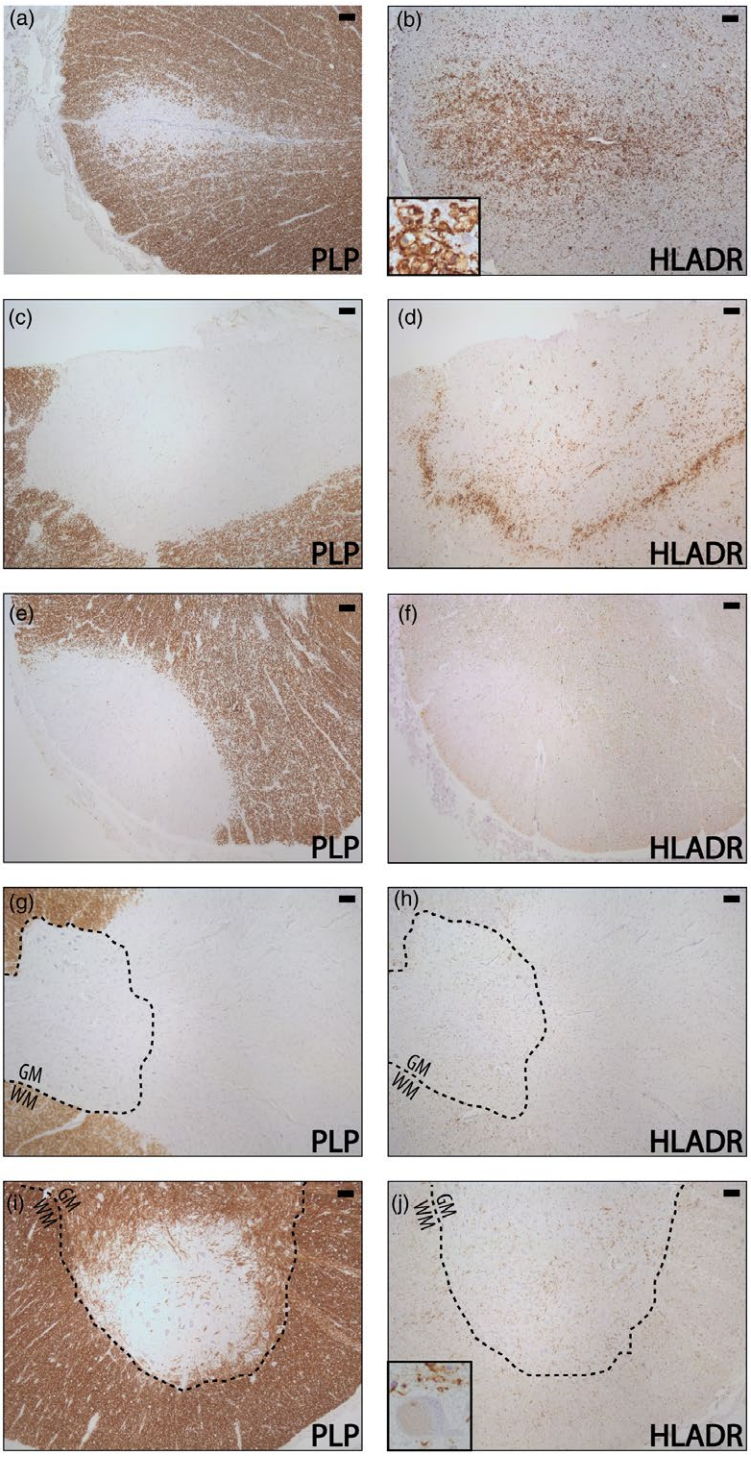

Fig. 2. White (WM) and grey matter (GM) spinal cord lesions. WM lesions were staged as active, chronic active or inactive based on the presence of demyelination and (foamy) microglia and/or macrophages as visualized by proteolipid protein (PLP) and human leucocyte antigen D-related (HLA-DR) staining. GM lesions were staged as type I and type II lesions based on WM/GM involvement. (a) Active lesion PLP staining. (b) Active lesion HLA-DR staining with a close-up of foamy microglia and/or macrophages. (c) Chronic active lesion PLP staining. (d) Chronic active lesion HLA-DR staining. (e) Inactive lesion PLP staining. (f) Inactive lesion HLA-DR staining. (g) Type I GM lesion PLP staining. (h) Type I GM lesion HLA-DR staining. (i) Type II GM lesion PLP staining. (j) Type II GM lesion HLA-DR staining with a close-up of a neurone surrounded by HLA-DR$^+$ microglia and/or macrophages. Where applicable, the borders between WM and GM are delineated with a dotted line. Scale bar in all pictures is 50 μm. Inserts are digitally enlarged.

in expression was observed in MS NAWM (Fig. 4b,g; $P = 0{\cdot}0173$), although this was not reflected in the WB studies where HSPB5 expression did not differ between brain and spinal cord CWM and NAWM. Relative to CWM, expression of HSPB5 was also increased significantly in active lesions (Fig. 4c,g; $P = 0{\cdot}0005$) and in the rim of chronic active lesions (Fig. 4d,g; $P = 0{\cdot}0169$), mainly in vimentin$^+$ astrocytes (insert Fig. 4c). Conversely, HSPB5 expression was not increased significantly in the centre of chronic active lesions (Fig. 4; $P = 0{\cdot}2581$) or in inactive lesions (Fig. 4f,g; $P = 0{\cdot}7581$), although here HSPB5$^+$vimentin$^+$ astrocytes were observed occasionally (insert Fig. 4e). While HSPB5 expression was observed in WM astrocytes, HSPB5 was not observed in GM astrocytes, with the exception of astrocytes in the immediate proximity of the central canal (data not shown). In CGM (Fig. 4h,i) and NAGM (Fig. 4h,j), oligodendrocyte lineage cells expressed HSPB5, while in demyelinated GM lesions (Fig. 4,k,l), HSPB5$^+$olig2$^+$ oligodendrocytes were observed rarely (data not shown). Neuronal expression of HSPB5 was not observed.

Morphologically distinct astrocytes express differentially phosphorylated HSPB5

Phosphorylation of HSPB5 at serine 59 (ser59) has been implicated recently in astrogliosis [26] prompting the evaluation of the different phosphorylated forms of HSPB5: serine 19 (ser19), serine 45 (ser45) and ser59 in the spinal cord (Fig. 4m,p). In CWM and CGM, cells with an oligodendrocyte-like morphology expressed all three variants of HSPB5, most prominently ser59 close to the nucleus, while only few ser19/45/59$^+$ cells with an

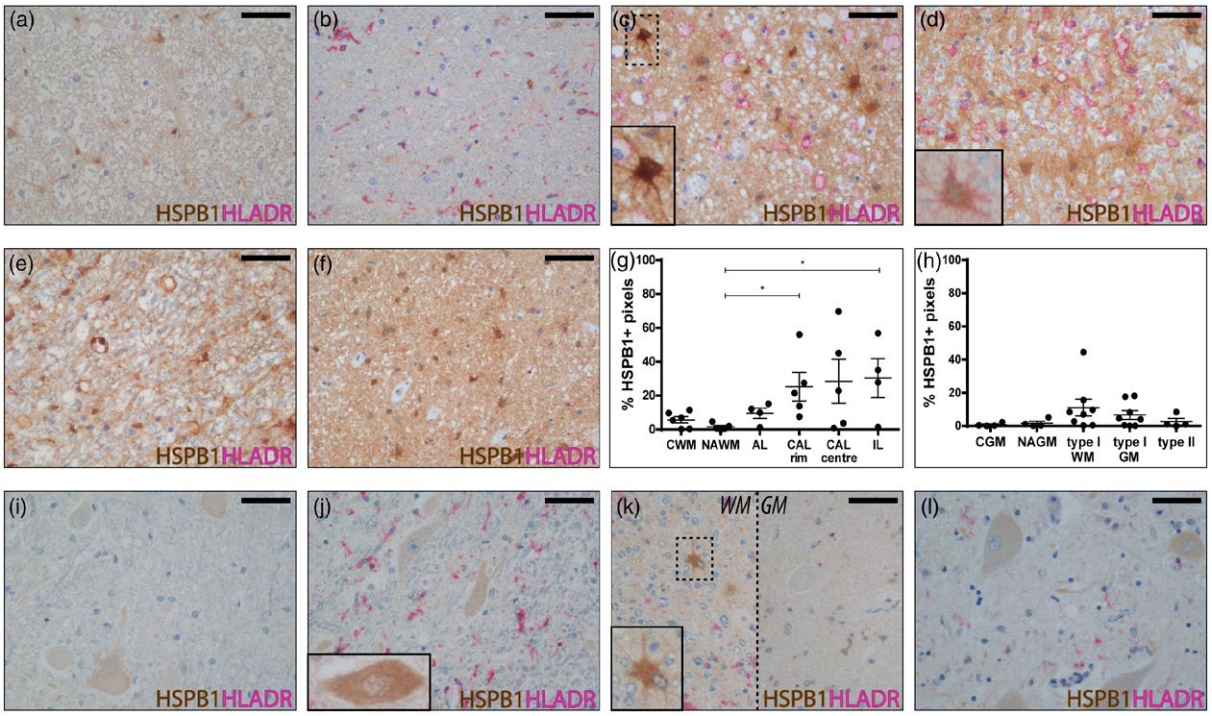

Fig. 3. Heat shock protein B (HSPB)1 expression in multiple sclerosis (MS) spinal cord lesions. Using immunohistochemistry (IHC), HSPB1 expression was evaluated in control white matter (CWM) (n = 6), normal-appearing white matter (NAWM) ($n = 5$), active lesions ($n = 4$), chronic active lesions ($n = 5$), inactive lesions ($n = 4$), control grey matter (CGM) ($n = 4$), normal-appearing grey matter (NAGM) ($n = 4$), type I GM lesions ($n = 8$) and type II GM lesions ($n = 4$). Representative lesions, stained for HSPB1 (brown) and human leucocyte antigen D-related (HLA-DR) (pink), are shown. HSPB1 expression was quantified by determining HSPB1$^+$ pixels using ImageJ. (a) HSPB1 expression in CWM. (b) HSPB1 expression in NAWM. (c) HSPB1 expression in an active lesion with a close-up of an HSPB1$^+$ (brown) cell with an astrocyte-like morphology. (d) HSPB1 expression in the rim of a chronic active lesion with an insert of a HSPB1$^+$ (brown) vimentin$^+$ (pink) astrocyte. (e) HSPB1 expression in the centre of a chronic active lesion. (f) HSPB1 expression in an inactive lesion. (g) Quantification HSPB1$^+$ pixels in WM lesions. (h) Quantification of HSPB1$^+$ pixels in GM lesions. (i) HSPB1 expression in CGM. (j) HSPB1 expression in NAGM with an insert of a HSPB1$^+$ neurone. (k) HSPB1 expression in WM and GM of a type I GM lesion with a close-up of a HSPB1$^+$ (brown) cell with an astrocyte-like morphology. (l) HSPB1 expression in a type II GM lesion. Statistically significant differences were evaluated by first comparing CWM/CGM and NAWM/NAGM with Student's *t*-test or Mann–Whitney *U*-test. No significant differences were found and NAWM/NAGM was next used to compare whether HSPB1 expression was up-regulated in GM/WM lesions using analysis of variance (ANOVA) and Dunnett's *post-hoc* test or Kruskal–Wallis test and Dunn's *post-hoc* test. Data are presented as mean with standard error of the mean. Significant data are presented (****$P < 0{\cdot}0001$, ***$P < 0{\cdot}001$, **$P < 0{\cdot}01$, *$P < 0{\cdot}05$). Scale bar in all pictures is 50 μm. Inserts are digitally enlarged.

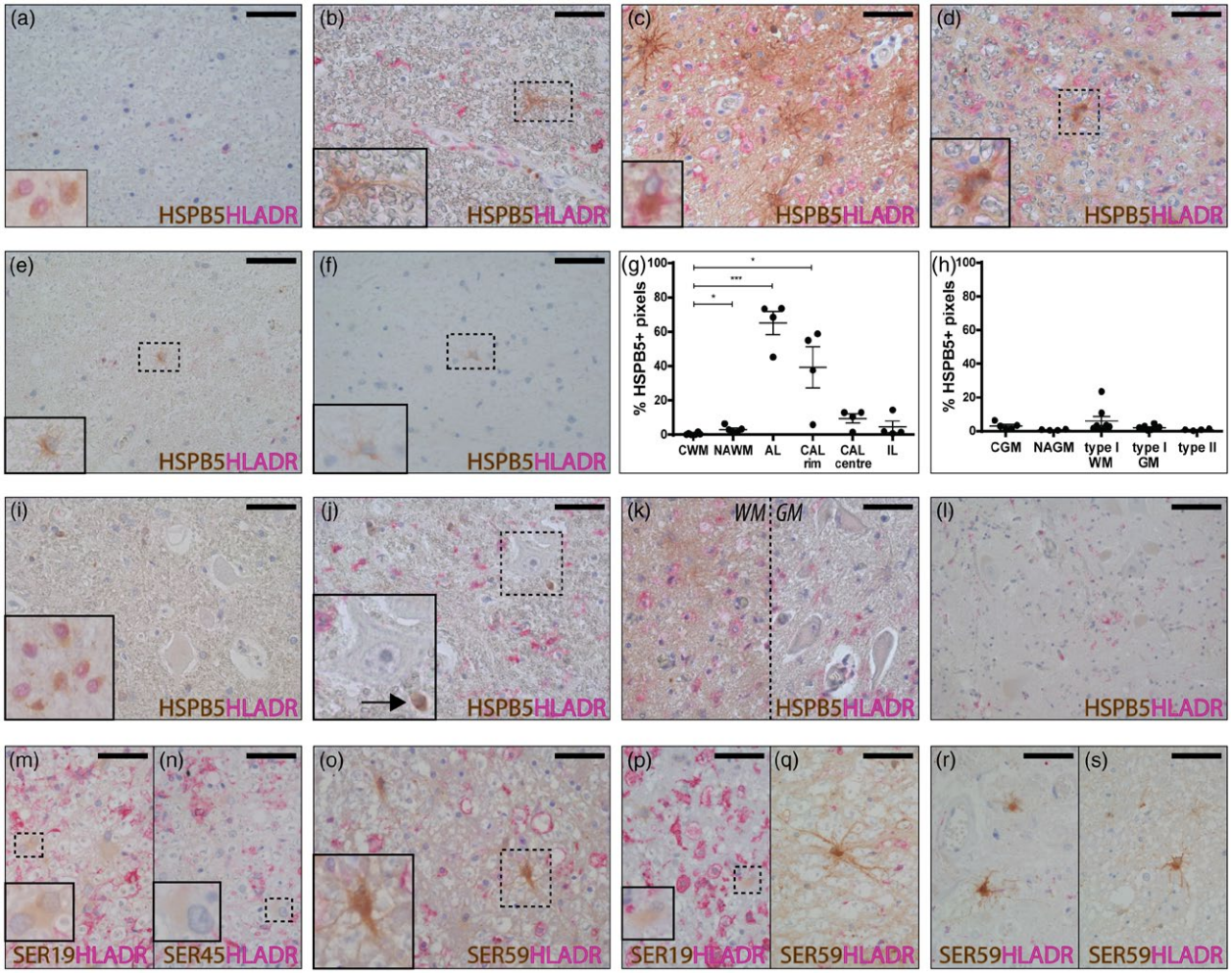

Fig. 4. Heat shock protein B (HSPB)5 expression in spinal cord lesions. Using immunohistochemistry (IHC), HSPB5 expression and expression of the different phosphorylated forms of HSPB5 (ser19, ser45, ser59) were evaluated in control white matter (CWM) ($n = 6$), normal-appearing white matter (NAWM) ($n = 5$), active lesions ($n = 4$), chronic active lesions ($n = 4$), inactive lesions ($n = 4$), control grey matter (CGM) ($n = 5$), normal-appearing grey matter (NAGM) ($n = 4$), type I GM lesions ($n = 8$) and type II GM lesions ($n = 4$). HSPB5 expression was quantified by determining HSPB5$^+$ pixels using ImageJ. Representative pictures stained for ser19/ser45/ser59 (brown) and human leucocyte antigen D-related (HLA-DR) (pink) are shown. (a) HSPB5 expression in CWM with an insert of HSPB5$^+$ (brown) olig2$^+$ (pink) oligodendrocytes. (b) HSPB5 expression in NAWM with a close-up of a HSPB5$^+$ (brown) cell with an astrocyte-like morphology. (c) HSPB5 expression in an active lesion with an insert of an HSPB5$^+$ (brown) vimentin$^+$ (pink) astrocyte. (d) HSPB5 expression in the rim of a chronic active lesion with a close-up of a HSPB5$^+$ (brown) cell with an astrocyte-like morphology. (e) HSPB5 expression in the centre of a chronic active lesion with a close-up of an HSPB5$^+$ (brown) cell with an astrocyte-like morphology. (f) HSPB5 expression in an inactive lesion with a close-up of an HSPB5$^+$ (brown) cell with an astrocyte-like morphology. (g) Quantification HSPB5$^+$ pixels in WM lesions. (h) Quantification HSPB5$^+$ pixels in GM lesions. (i) HSPB5 expression in CGM with an insert of HSPB5$^+$ (brown) olig2$^+$ (pink) oligodendrocytes. (j) HSPB5 expression in NAGM with a close-up (insert) of a neuron and a HSPB5$^+$ (brown) cell that morphologically resembles an oligodendrocyte (arrow). (k) HSPB5 expression in WM and GM of a type I GM lesion. (l) HSPB5 expression in a type II GM lesion. (m) Ser19 expression in an active lesion with a close-up of a ser19$^+$ cell with an astrocyte-like morphology. (n) Ser45 expression in an active lesion with a close-up of a ser45$^+$ cell with an astrocyte-like morphology. (o) Ser59 expression in an active lesion with a close-up of a ser59$^+$ cell with an astrocyte-like morphology. (p) Ser19 expression in the rim of a chronic active lesion with a close-up of a ser19$^+$ cell with an astrocyte-like morphology. (q) Ser59 expression in the rim of a chronic active lesion. (r) Ser59 expression in the centre of a chronic active lesion. (s) Ser59 expression in an inactive lesion. Statistically significant differences were evaluated by first comparing CWM/CGM and NAWM/NAGM with Student's *t*-test or Mann–Whitney *U*-test. If significant differences were found, NAWM/NAGM, and otherwise CWM/CGM, was next used to compare whether HSPB5 expression was up-regulated in GM/WM lesions using analysis of variance (ANOVA) and Dunnett's *post-hoc* test or Kruskal–Wallis test and Dunn's *post-hoc* test. Data are presented as mean with standard error of the mean. Significant data are presented (****$P < 0{\cdot}0001$, ***$P < 0{\cdot}001$, **$P < 0{\cdot}01$, *$P < 0{\cdot}05$). Scale bar in all pictures is 50 μm. Inserts are digitally enlarged.

astrocyte-like morphology were observed (data not shown). In active lesions, ser19 expression (Fig. 4m), and occasionally ser45 expression (Fig. 4n), were observed in the soma of cells with an astrocyte-like appearance and a hypertrophic morphology, while ser59 (Fig. 4o) was up-regulated highly in the cell body and processes of astrocyte-like cells with a ramified appearance. In the rim of chronic active lesions, low ser19 expression (Fig. 4p) and high ser59 expression (Fig. 4q) was observed, while in the centre of chronic active lesions (Fig. 4r) and in inactive lesions (Fig. 4s), only ser59 was found occasionally in ramified astrocytes. In active lesions and the rim of chronic active lesions all three variants were also detected in foamy macrophages in blood vessels (data not shown).

Expression of HSPB6 and HSPB8 is not altered in spinal cord lesions

HSPB6 (Fig. 5a,b) and HSPB8 (Fig. 5I,j) expression was observed in astrocyte-like cells in CWM and NAWM. Although several active lesions (Fig. 5d) and chronic active lesions (data not shown) revealed HSPB6 expression in astrocytes, as confirmed by double-staining with vimentin (insert Fig. 5c), HSPB6 expression in MS lesions was not significantly different from NAWM (Fig. 5d). Similarly, HSPB8 expression was detected in HSPB8$^+$vimentin$^+$ astrocytes (insert Fig. 5k) in three of four inactive lesions (Fig. 5k), but no significant differences were detected (Fig. 5k; P = 0·2853). Expression of HSPB6 and HSPB8 was not observed in oligodendrocyte lineage cells (data not shown). In CGM and NAGM, expression of HSPB6 (Fig. 5e,f) and HSPB8 (Fig. 5m,n) was observed in GM astrocytes. No changes in HSPB6 and HSPB8 expression were observed in type I (Fig. 5g,h,o,p) or in type II GM lesions (data not shown).

HSP16.2 expression is increased in NAGM and type I GM lesions

HSP16.2 expression was observed in cells with an astrocyte-like morphology in CWM (Fig. 5q), NAWM (Fig. 5r) and MS lesions (Fig. 5s,t). In active lesions (Fig. 5s,t; P = 0·8781), HSP16.2$^+$vimentin$^+$ astrocytes were present (insert, Fig. 5s), although HSP16.2 expression was not significantly different from NAWM. While HSP16.2 expression was observed only occasionally in GM astrocytes, neurones throughout the GM expressed HSP16.2 in a synaptic pattern in CGM (Fig. 5u), NAGM (Fig. 5v) and GM lesions (Fig. 5w,x). Compared to CGM, HSP16.2 expression was significantly higher in NAGM (Fig. 5v,x; P = 0·0244) and type I GM lesions (Fig. 5w,x; P = 0·0329), although no differences were detected with WB.

Discussion

Spinal cord pathology is a crucial factor contributing to disease progression in MS. Although there is high regional heterogeneity in the CNS, possibly influencing local responses to pharmacological agents, pathology studies focus frequently on brain pathology, neglecting the clinical relevance of MS lesions arising outside the brain. in this study, we compared HSPBs and HSP16.2 levels in brain and spinal cord WM and GM, and further investigated HSP expression in WM and GM spinal cord lesions. We show that in the spinal cord, similar to the brain, astrocytes are the main source of HSPBs, but that basal levels of HSPB1, HSPB6 and HSPB8 are increased markedly in the spinal cord, more prominently in WM, and that expression of HSPB5 and HSP16.2 in spinal cord lesions is subtly different from the brain.

Using WB and IHC, our studies reveal that spinal cord astrocytes have higher basal expression of HSPB1, HSPB6 and HSPB8 than brain astrocytes. Throughout the CNS, astrocytes perform a wide variety of functions, including facilitation of neuronal/axonal growth, clearing waste products, regulation of glutamate transport, controlling blood–brain barrier integrity and enabling scar formation in reaction to tissue injury [3,27]. Regional astrocyte subsets are specialized morphologically, molecularly and functionally to optimally function in their microenvironment [28,29]. A recent study showed that levels of glial fibrillary acid protein (GFAP) are higher in both in WM and GM in murine spinal cord compared to brain, and increased in cultured spinal cord astrocytes compared to cortical astrocytes [30]. GFAP is the principal intermediate filament cytoskeletal protein in adult astrocytes, important in providing cell shape, strength and motility [31]. Increased levels of GFAP (and possibly other cytoskeletal proteins) in spinal cord astrocytes may be advantageous as, due to anatomical localization and increased mobility, the spinal cord is subjected to far greater mechanical stress than the brain. HSPBs interact with the cytoskeleton by preventing aggregation, influencing assembly and providing stabilization of cytoskeletal proteins, such as GFAP [32]. The relatively high levels of HSPB1, HSPB6 and HSPB8 in WM (and GM) spinal cord astrocytes as we show here are probably necessary for proper functioning of the cytoskeleton. HSPB1 associates with GFAP under non-stressed conditions and upon heat shock, inhibiting GFAP assembly [33]. To our knowledge, HSPB6 and HSPB8 are not known to interact with GFAP, although both HSPs are involved in assembly/disassembly dynamics of the microfilament actin [34,35], another astrocyte cytoskeletal protein [36]. Of note, HSPB5 (and HSP16.2) expression was not more abundant in spinal cord,

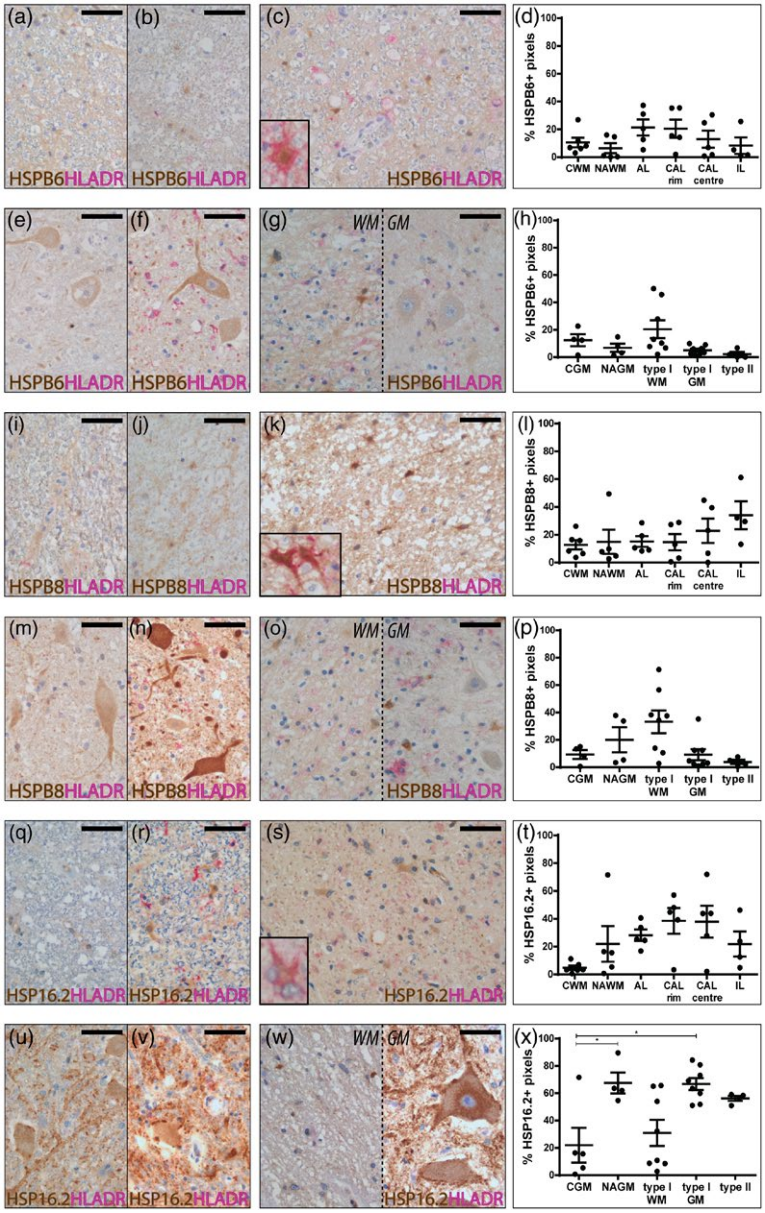

Fig. 5. Heat shock protein B (HSPB)6, HSPB8 and HSP16.2 expression in multiple sclerosis (MS) spinal cord lesions. Using immunohistochemistry (IHC), HSPB6, HSPB8 and HSP16.2 expression was evaluated in control white matter (CWM) ($n = 6$), normal-appearing white matter (NAWM) ($n = 5$), active lesions ($n = 5$), chronic active lesions ($n = 5$), inactive lesions ($n = 4$), CGM ($n = 4$–5), NAGM ($n = 4$), type I GM lesions ($n = 8$) and type II GM lesions ($n = 4$). Representative lesions, stained for HSPB6/HSPB8/HSP16.2 (brown) and human leucocyte antigen D-related (HLA-DR) (pink), are shown. HSPB6/HSPB8/HSP16.2 expression was quantified by determining HSP+ pixels using ImageJ. (a) HSPB6 expression in CWM. (b) HSPB6 expression in NAWM. (c) HSPB6 expression in an active lesion with an insert of an HSPB6+ (brown) vimentin+ (pink) astrocyte. (d) Quantification of HSPB6+ pixels in WM lesions. (e) HSPB6 expression in control grey matter (CGM). (f) HSPB6 expression in normal-appearing grey matter (NAGM. (g) HSPB6 expression in WM and GM of a type I GM lesion. (h) Quantification HSPB6+ pixels in GM lesions. (i) HSPB8 expression in CWM. (j) HSPB8 expression in NAWM. (k) HSPB8 expression in an inactive lesion with an insert of a HSPB8+ (brown) vimentin+ (pink) astrocyte. (l) Quantification of HSPB8+ pixels in WM lesions. (m) HSPB8 expression CGM. (n) HSPB8 expression in NAGM. (o) HSPB8 expression in WM and GM of a type I GM lesion. (p) Quantification of HSPB8+ pixels in GM lesions. (q) HSP16.2 expression in CWM. (r) HSP16.2 expression in NAWM. (s) HSP16.2 expression in an active lesion with an insert of a HSP16.2+ (brown) vimentin+ (pink) astrocyte. (t) Quantification of HSP16.2+ pixels in WM lesions. (u) HSP16.2 expression in CGM. (v) HSP16.2 expression in NAGM. (w) HSP16.2 expression in WM and GM of a type I GM lesion. (x) Quantification of HSP16.2 expression in GM lesions. Statistically significant differences were evaluated by first comparing CWM/CGM and NAWM/NAGM with Student's *t*-test or Mann–Whitney *U*-test. If no significant differences were found, NAWM/NAGM, and otherwise CWM/CGM, was next used to compare whether HSP expression was up-regulated in GM/WM lesions using analysis of variance (ANOVA) and Dunnett's *post-hoc* test or Kruskal–Wallis test and Dunn's *post-hoc* test. Data are presented as mean with standard error of the mean. Significant data are presented (****$P < 0{\cdot}0001$, ***$P < 0{\cdot}001$, **$P < 0{\cdot}01$, *$P < 0{\cdot}05$). Scale bar in all pictures is 50 μm. Inserts are digitally enlarged.

underscoring the concept that HSPBs are structurally related, but functionally highly heterogeneous [37]. HSPB5 is well known to bind to GFAP, inhibiting GFAP fibril formation *in vitro* [38] and *in vivo* [39], raising the question of why HSPB5 levels are not up-regulated. As HSPB1, HSPB6 and HSPB8 are involved in many cellular processes besides cytoskeleton maintenance, including proteostasis, cell division and protection against oxidative radicals [37], increased spinal cord levels of these HSPBs may not (only) signify cytoskeletal heterogeneity, but reflect other differences between the spinal cord and the brain, such as greater remyelinating capacity [19], relatively higher permeability of the blood–spinal cord barrier [4], mitochondrial differences [40,41], higher metabolic requirements or increased cell turnover.

MS spinal cord lesions are markedly different from previous studies in brain lesions [24] with regard to HSP16.2 and HSPB5 expression, illustrating that the spinal cord and brain do not only differ in healthy conditions, but also in their reactions to tissue injury. A previous study by our group evaluated (small) HSP expression upon MS lesion development in the brain and reported increased expression of HSPB1, HSPB6 and HSPB8 in MS lesions, mainly in the centre of chronic active lesions [24]. Although in the spinal cord only HSPB1 expression was significantly different in the rim of chronic active lesions and inactive lesions, the disparity might be due partly to study design. First, the study in MS brain quantified HSP expression relative to the total number of cells [24], thus underestimating HSP levels per cell as well as HSP levels in active lesions and the rim of chronic active lesions in case large numbers of microglia and macrophages are present which do not express HSPs. Secondly, the statistical power of the current study is limited by the availability of spinal cord tissues.

Contrary to the investigated HSPBs, which are expressed mainly by astrocytes (and HSPB5 by oligodendrocyte lineage cells), HSP16.2 expression was found to be most prominent in spinal cord neurones, where it was expressed in the cytosol and on the neuronal membrane in a synaptic pattern in CGM, NAGM and GM lesions. Quantification of IHC found that neuronal HSP16.2 expression was significantly more intense in NAGM and type I GM lesions compared to CGM, unlike that seen previously in cortical lesions, where no differences in HSP16.2 expression were found [24]. However, while no differences were detected in HSP16.2 levels between MS patients and controls using WB, complexes of HSP16.2 were observed in the brain GM but not the spinal cord. Alternatively, differences observed using IHC, but not WB, might be due to age differences, as for the IHC study MS patients with spinal cord lesions were selected which were, on average, 12 years younger than the available controls. HSP16.2 (also known as HSPC034, IFT25, PP25 and C1orf41) has debatably been proposed as the eleventh member of the HSPB family (HSPB11) [42]. Although HSP16.2 functions as a chaperone protein and has anti-apoptotic properties [42], it does not contain an α-crystallin domain, which is highly conserved in HSPB1-10, indicating that these proteins are evolutionarily unrelated [43], thus possibly explaining our deviant results for HSP16.2. Although HSP16.2 is known to be involved in hedgehog signalling [44], can partially supress amyloid toxicity in a *Caenorhabditis elegans* model of Alzheimer's disease [45] and is associated with histological tumour grade in malignant brain tumours [46], its exact function in (spinal cord) neurones remains to be determined.

In the spinal cord, we show that HSPB5 (αB-crystallin) is increased in active inflammatory lesions, while it is virtually absent in inactive lesions in the spinal cord. This is in contrast to a previous report showing that HSPB5 is up-regulated in ~45% of astrocytes in early active, late active and inactive brain lesions [25]. Although these differences could be due to staining techniques, the differential expression of HSPB5 possibly indicates differences in spinal cord astrocyte responses to demyelination. In support of this, an identical mechanical insult induces similar levels of astrocyte reactivity in the brain and spinal cord, as measured by increased GFAP staining intensity, but in the spinal cord the astrocyte response develops more rapidly and declines earlier compared to the brain [20]. Furthermore, a comparison of astrocyte responses in brain and spinal cord upon lysolecithin-induced demyelination revealed that 14 days post-injection GFAP reactivity is markedly higher in the spinal cord compared to brain [30].

By acting as an extracellular signal to cells, HSPB are reported to induce innate immune responses. In MS, elevated expression of HSPB5 in MS may influence inflammation, as HSPB5 activates microglia via Toll-like receptor (TLR)-2 and CD14 [47,48]. Other HSPBs, e.g. HSPB1 and HSPB8, have also been reported to act as agonists of TLR signalling [49–51], and thus expression of HSPBs are likely to influence inflammatory responses in the CNS. Thus the differential expression of HSPB and HSP16.2 in the CNS may well influence the pathology and clinical outcome in MS.

In inflammatory spinal cord lesions, stellate astrocytes express HSPB5 ser59 prominently, while hypertrophic astrocytes express HSPB5 ser19 and, to a lesser extent, HSPB5 ser45. HSPB5 is involved in a multitude of cellular processes by interacting with more than 90 different proteins, necessitating mechanisms to post-translationally regulate HSPB5 activity, such as phosphorylation [52,53].

HSPB5 can be phosphorylated at three different serine residues (ser19, ser45 and ser59). Although the different phosphorylated forms show functional overlap, HSPB5 phosphorylation at ser19 and ser45 is especially important in cell cycle regulation, while ser59 is involved mainly in inflammatory pathways [26,53]. Recently, phosphorylation of HSPB5 at ser59 has been implicated in astrogliosis [26]. In active brain MS lesions expression of HSPB5 ser59, but not HSPB5 ser45, is increased in reactive astrocytes [26], unlike in the spinal cord, illustrating heterogeneity in astrocyte populations and astrocyte responses to demyelinating injury across the CNS.

To date, limited data are available on the expression profiles of HSPs during (spinal cord) lesion development in MS lesions, even though such profiles may hold important clues to molecular factors involved in the disease process. High levels of HSPB expression in the spinal cord and differential expression of (small) HSPs by astrocytes and neurones in spinal cord lesions illustrate differences between brain and spinal cord in normal conditions and upon demyelination. As regional heterogeneity probably influences the pathology of MS lesions as well as local effectiveness of pharmacological agents, research elucidating differences between brain and spinal cord may ultimately help to increase the effectiveness of (current) therapies on the debilitating spinal cord lesions.

Acknowledgements

Fight for Sight UK (1584/1585) funded the HSPB5 phosphorylation experiments; otherwise, we did not receive any specific grant from funding agencies in the public, commercial or not-for-profit sectors.

Disclosures

The authors declare no conflicts of interest.

References

1 Compston A, Coles A. Multiple sclerosis. Lancet 2002; **359**:1221–31.

2 McCarthy MM. Location, location, location: microglia are where they live. Neuron [internet] 2017; **95**:233–5. Available at: https://www.ncbi.nlm.nih.gov/pubmed/28728016 (accessed 7 May 2018).

3 Bayraktar OA, Fuentealba LC, Alvarez-Buylla A, Rowitch DH. Astrocyte development and heterogeneity. Cold Spring Harb Perspect Biol 2014; **7**:a020362.

4 Wilhelm I, Nyúl-Tóth Á, Suciu M, Hermenean A, Krizbai IA. Heterogeneity of the blood–brain barrier. Tissue Barriers [internet] 2016; **4**:e1143544. Available at: https://www.ncbi.nlm.nih.gov/pubmed/27141424 (accessed 7 May 2018).

5 Zhang B, Gensel JC. Is neuroinflammation in the injured spinal cord different than in the brain? Examining intrinsic differences between the brain and spinal cord. Exp Neurol [internet] 2014; **258**:112–20. Available at: https://www.ncbi.nlm.nih.gov/pubmed/25017892 (accessed 7 May 2018).

6 Scheff SW, Sullivan PG. Cyclosporin a significantly ameliorates cortical damage following experimental traumatic brain injury in rodents. J Neurotrauma [internet] 1999; **16**:783–92. Available at: https://www.ncbi.nlm.nih.gov/pubmed/10521138 (accessed 22 May 2018).

7 Rabchevsky AG, Fugaccia I, Sullivan PG, Scheff SW. Cyclosporin a treatment following spinal cord injury to the rat: behavioral effects and stereological assessment of tissue sparing. J Neurotrauma [internet] 2001; **18**:513–22. Available at: https://www.ncbi.nlm.nih.gov/pubmed/11393254 (accessed 22 May 2018).

8 Bot JCJ, Barkhof F, Polman CH*et al*. Spinal cord abnormalities in recently diagnosed MS patients: added value of spinal MRI examination. Neurology [internet] 2004; **62**:226–33. Available at: https://www.ncbi.nlm.nih.gov/pubmed/14745058 (accessed 7 May 2018).

9 Conrad BN, Barry RL, Rogers BP*et al*. Multiple sclerosis lesions affect intrinsic functional connectivity of the spinal cord. Brain [internet] 2018; 141:1650–64. Available at: https://www.ncbi.nlm.nih.gov/pubmed/29648581 (accessed 7 May 2018).

10 Compston A. McAlpine's multiple sclerosis. London: Churchill Livingstone Elsevier, 2005.

11 Bramow S, Frischer JM, Lassmann H*et al*. Demyelination versus remyelination in progressive multiple sclerosis. Brain [internet] 2010; **133**:2983–98. Available at: https://www.ncbi.nlm.nih.gov/pubmed/20855416 (accessed 7 May 2018).

12 Li Z, Lu C, Wang Y, Hashizume Y, Yoshida M. Heterogeneity of spinal cord pathology in multiple sclerosis and variants: a study of postmortem specimen from 13 Asian patients. Neurol Asia [internet] 2006; **11**:111–21. Available at: https://www.neurology-asia.org/articles/20062_111.pdf (accessed 7 May 2018).

13 Gilmore CP, DeLuca GC, Bö L*et al*. Spinal cord neuronal pathology in multiple sclerosis. Brain Pathol [internet] 2009; **19**:642–9. Available at: https://www.ncbi.nlm.nih.gov/pubmed/19170682 (accessed 2 October 2017).

14 Petrova N, Carassiti D, Altmann DR, Baker D, Schmierer K. Axonal loss in the multiple sclerosis spinal cord revisited. Brain Pathol [internet] 2017; 28:334–48. Available at: https://www.ncbi.nlm.nih.gov/pubmed/28401686 (accessed 2 October 2017).

15 Ganter P, Prince C, Esiri MM. Spinal cord axonal loss in multiple sclerosis: a post-mortem study. Neuropathol Appl Neurobiol [internet] 1999; **25**:459–67. Available at: https://www.ncbi.nlm.nih.gov/pubmed/10632896 (accessed 2 October 2017).

16 Androdias G, Reynolds R, Chanal M, Ritleng C, Confavreux C, Nataf S. Meningeal T cells associate with diffuse axonal loss in multiple sclerosis spinal cords. Ann Neurol [internet] 2010; **68**:465–76. Available at: https://www.ncbi.nlm.nih.gov/pubmed/20687208 (accessed 7 May 2018).

17 Gilmore CP, Donaldson I, Bo L, Owens T, Lowe J, Evangelou N. Regional variations in the extent and pattern of grey matter demyelination in multiple sclerosis: a comparison between the

cerebral cortex, cerebellar cortex, deep grey matter nuclei and the spinal cord. J Neurol Neurosurg Psychiatry 2009; **80**:182–7.

18 Schirmer L, Antel JP, Brück W, Stadelmann C. Axonal loss and neurofilament phosphorylation changes accompany lesion development and clinical progression in multiple sclerosis. Brain Pathol [internet] 2011; **21**:428–40. Available at: https://doi.wiley.com/10.1111/j.1750-3639.2010.00466.x (accessed 7 May 2018).

19 Luchetti S, Fransen NL, vanEden CG, Ramaglia V, Mason M, Huitinga I. Progressive multiple sclerosis patients show substantial lesion activity that correlates with clinical disease severity and sex: a retrospective autopsy cohort analysis. Acta Neuropathol [internet] 2018; **135**:511–28. Available at: https://link.springer.com/10.1007/s00401-018-1818-y (accessed 28 May 2018).

20 Schnell L, Fearn S, Klassen H, Schwab ME, Perry VH. Acute inflammatory responses to mechanical lesions in the CNS: differences between brain and spinal cord. Eur J Neurosci [internet] 1999; **11**:3648–58. Available at: https://www.ncbi.nlm.nih.gov/pubmed/10564372 (accessed 2 October 2017).

21 Batchelor PE, Tan S, Wills TE, Porritt MJ, Howells DW.Comparison of Inflammation in the brain and spinal cord following mechanical injury. J Neurotrauma [internet] 2008; **25**:1217–25. Available at: https://www.ncbi.nlm.nih.gov/pubmed/18986223 (accessed 7 May 2018).

22 Richter K, Haslbeck M, Buchner J. The heat shock response: life on the verge of death. Mol Cell [internet] 2010; **40**:253–66. Available at: https://www.ncbi.nlm.nih.gov/pubmed/20965420 (accessed 8 May 2018).

23 Dulle JE, Fort PE.Crystallins and neuroinflammation: the glial side of the story. Biochim Biophys Acta [internet] 2016 Jan; **1860**:278–86. Available at: https://www.ncbi.nlm.nih.gov/pubmed/26049079 (accessed 8 May 2018).

24 Peferoen LAN, Gerritsen WH, Breur M*et al.* Small heat shock proteins are induced during multiple sclerosis lesion development in white but not grey matter. Acta Neuropathol Commun [internet] 2015; **3**:87. Available at: https://www.ncbi.nlm.nih.gov/pmc/articles/PMC4688967 (accessed 22 Dec 2015).

25 Bajramovic JJ, Lassmann H, van Noort JM. Expression of alphaB-crystallin in glia cells during lesional development in multiple sclerosis. J Neuroimmunol 1997; **78**:143–51.

26 Kuipers HF, Yoon J, van Horssen J *et al.* Phosphorylation of alphaB-crystallin supports reactive astrogliosis in demyelination. Proc Natl Acad Sci USA 2017; **114**:E1745–54.

27 Sofroniew MV, Vinters HV. Astrocytes: biology and pathology. Acta Neuropathol [internet] 2010; **119**:7–35. Available at: https://www.ncbi.nlm.nih.gov/pmc/articles/PMC2799634. (accessed 10 December 2009).

28 Emsley JG, Macklis JD. Astroglial heterogeneity closely reflects the neuronal-defined anatomy of the adult murine CNS. Neuron Glia Biol; **2**:175–86.

29 Nair A, Frederick TJ, Miller SD. Astrocytes in multiple sclerosis: a product of their environment. Cell Mol Life Sci [internet] 2008; **65**:2702–20. Available at: https://www.ncbi.nlm.nih.gov/pmc/articles/PMC2858316 (accessed 2 September 2008).

30 Yoon H, Walters G, Paulsen AR, Scarisbrick IA.Astrocyte heterogeneity across the brain and spinal cord occurs developmentally, in adulthood and in response to demyelination. PLOS ONE [internet] 2017; **12**:e0180697. Available at: https://www.ncbi.nlm.nih.gov/pubmed/28700615 (accessed 2 October 2017).

31 Middeldorp J, Hol EM.GFAP in health and disease. Prog Neurobiol [internet] 2011; **93**:421–43. Available at: https://www-sciencedirect-com.proxy-ub.rug.nl/science/article/pii/S0301008211000062?_rdoc = 1&_fmt = high&_origin = gateway&_docanchor = &md5 = b8429449ccfc9c30159a5f9aeaa92ffb (accessed 21 May 2018).

32 Wettstein G, Bellaye PS, Micheau O, Bonniaud P.Small heat shock proteins and the cytoskeleton: an essential interplay for cell integrity? Int J Biochem Cell Biol [internet] 2012; **44**:1680–6. Available at: https://www.ncbi.nlm.nih.gov/pubmed/22683760 (accessed 30 September 2017).

33 Perng MD, Cairns L, van den IJssel P, Prescott A, Hutcheson AM, Quinlan RA. Intermediate filament interactions can be altered by HSP27 and alphaB-crystallin. J Cell Sci [internet] 1999; **112**:2099–112. Available at: https://www.ncbi.nlm.nih.gov/pubmed/10362540 (accessed 21 May 2018).

34 Dreiza CM, Brophy CM, Komalavilas P*et al.* Transducible heat shock protein 20 (HSP20) phosphopeptide alters cytoskeletal dynamics. FASEB J [internet] 2005; **19**:261–3. Available at: https://www.fasebj.org/doi/10.1096/fj.04-2911fje (accessed 21 May 2018).

35 Fuchs M, Luthold C, Guilbert SM*et al.* A role for the chaperone complex BAG3–HSPB8 in actin dynamics, spindle orientation and proper chromosome segregation during mitosis. PLOS Genet [internet] 2015; **11**:e1005582. Available at: https://www.ncbi.nlm.nih.gov/pubmed/26496431 (accessed 21 May 2018).

36 Lecain E, Alliot F, Laine MC, Calas B, Pessac B.Alpha isoform of smooth muscle actin is expressed in astrocytes *in vitro* and *in vivo*. J Neurosci Res [internet] 1991;**28**:601–6. Available at: https://doi.wiley.com/10.1002/jnr.490280417 (accessed 21 May 2018).

37 Kampinga HH, Garrido C. HSPBs: small proteins with big implications in human disease. Int J Biochem Cell Biol 2012; **44**:1706–10.

38 Nicholl ID, Quinlan RA. Chaperone activity of alpha-crystallins modulates intermediate filament assembly. EMBO J [internet] 1994; **13**:945–53. Available at: https://www.ncbi.nlm.nih.gov/pubmed/7906647 (accessed 21 May 2018).

39 Hagemann TL, Boelens WC, Wawrousek EF, Messing A.Suppression of GFAP toxicity by αB-crystallin in mouse models of Alexander disease. Hum Mol Genet [internet] 2009; **18**:1190–9. Available at: https://academic.oup.com/hmg/article-lookup/doi/10.1093/hmg/ddp013 (accessed 30 September 2017).

40 Sullivan PG, Rabchevsky AG, Keller JN*et al.* Intrinsic differences in brain and spinal cord mitochondria: Implication for therapeutic interventions. J Comp Neurol [internet] 2004; **474**:524–34. Available at: https://doi.wiley.com/10.1002/cne.20130 (accessed 22 May 2018).

41 Panov AV, Kubalik N, Zinchenko N*et al*. Metabolic and functional differences between brain and spinal cord mitochondria underlie different predisposition to pathology. Am J Physiol Regul Integr Comp Physiol [internet] 2011; **300**:R844–54. Available at: https://www.physiology.org/doi/10.1152/ajpregu.00528.2010 (accessed 22 May 2018).

42 Bellyei S, Szigeti A, Pozsgai E*et al*. Preventing apoptotic cell death by a novel small heat shock protein. Eur J Cell Biol [internet] 2007; **86**:161–71. Available at: https://www.ncbi.nlm.nih.gov/pubmed/17275951 (accessed 22 May 2018).

43 Kappé G, Boelens WC, DeJong WW.Why proteins without an a-crystallin domain should not be included in the human small heat shock protein family HSPB. Available at: https://www.ncbi.nlm.nih.gov/pmc/articles/PMC3082639/pdf/12192_2009_Article_155.pdf (accessed 21 May 2018).

44 Keady BT, Samtani R, Tobita K*et al*. IFT25 Links the signal-dependent movement of hedgehog components to intraflagellar transport. Available at: https://www.ncbi.nlm.nih.gov/pmc/articles/PMC3366633/pdf/nihms374784.pdf (accessed 22 May 2018).

45 Fonte V, Kipp DR, Yerg Iii J*et al*. Suppression of *in vivo* β-amyloid peptide toxicity by overexpression of the HSP-16.2 small chaperone protein. J Biol Chem 2007; 283:784–91. Available at: https://www.jbc.org/content/283/2/784.full.pdf (accessed 22 May 2018).

46 Pozsgai E, Gomori E, Szigeti A*et al*. Correlation between the progressive cytoplasmic expression of a novel small heat shock protein (Hsp16.2) and malignancy in brain tumors. BMC Cancer [internet] 2007; **7**:233. Available at: https://www.biomedcentral.com/1471-2407/7/233 (accessed 22 May 2018).

47 van Noort JM, Bsibsi M, Gerritsen WH *et al*. Alphab-crystallin is a target for adaptive immune responses and a trigger of innate responses in preactive multiple sclerosis lesions. J Neuropathol Exp Neurol 2010; **69**:694–703.

48 van Noort JM, Bsibsi M, Nacken PJ *et al*. Activation of an immune-regulatory macrophage response and inhibition of lung inflammation in a mouse model of COPD using heat-shock protein alpha B-crystallin-loaded PLGA microparticles. Biomaterials 2013; **34**:831–40.

49 Roelofs MF, Boelens WC, Joosten LAB*et al*. Identification of small heat shock protein B8 (HSP22) as a novel TLR4 ligand and potential involvement in the pathogenesis of rheumatoid arthritis. J Immunol [internet] 2006; **176**:7021–7. Available at: https://www.ncbi.nlm.nih.gov/pubmed/16709864 (accessed 31 May 2018).

50 Thuringer D, Jego G, Wettstein G*et al*. Extracellular HSP27 mediates angiogenesis through Toll-like receptor 3. FASEB J [internet] 2013; **27**:4169–83. Available at: https://www.ncbi.nlm.nih.gov/pubmed/23804239 (accessed 31 May 2018).

51 van Noort JM, Bsibsi M, Nacken P, Gerritsen WH, Amor S.The link between small heat shock proteins and the immune system. Int J Biochem Cell Biol [internet] 2012; **44**:1670–9. Available at: https://www.ncbi.nlm.nih.gov/pubmed/22233974 (accessed 31 May 2018).

52 Arrigo A-P, Gibert B.Protein interactomes of three stress inducible small heat shock proteins: HspB1, HspB5 and HspB8. Int J Hyperth [internet] 2013; **29**:409–22. Available at: https://www.ncbi.nlm.nih.gov/pubmed/23697380 (accessed 22 May 2018).

53 Bakthisaran R, Akula KK, Tangirala R, Rao CM.Phosphorylation of αB-crystallin: role in stress, aging and patho-physiological conditions. Biochim Biophys Acta [internet] 2016; **1860**:167–82. Available at: https://linkinghub.elsevier.com/retrieve/pii/S0304416515002597 (accessed 22 May 2018).

Supporting Information

Additional supporting information may be found in the online version of this article at the publisher's web site:

Fig. S1. HSP levels in controls and MS patients. HSPB1, HSPB5, HSPB6, HSPB8 and HSP16.2 protein levels in brain WM/GM and spinal cord WM/GM of controls (n = 8) and MS patients (n = 8) were determined using Western blotting and quantified with Scion Image. Actin was used as a loading control. Values are normalized to a reference sample. (a) Quantification HSPB1 protein levels in controls and MS patients. (b) Quantification HSPB6 protein levels in controls and MS patients. (c) Quantification HSPB8 protein levels in controls and MS patients. (d) Quantification HSPB5 protein levels in controls and MS patients. (e) Quantification HSP16.2 protein levels in controls and MS patients. To compare HSP levels between MS patients and controls, WM and GM and brain and spinal cord, ANOVA or Kruskal–Wallis test and *post-hoc* testing with Sidak's or Dunn's multiple comparisons test was performed. Data are presented as mean with standard error of the mean. Significant data are presented (****P < 0·0001, ***P < 0·001, **P < 0·01, *P < 0·05).

Fig. S2. HSP16.2 expression in brain and spinal cord. HSP16.2 protein levels in brain WM/GM and spinal cord (SPC) WM/GM of controls (n = 8) and MS patients (n = 8) were determined using Western blotting. A representative blot with two controls and one MS patient is shown. The reference sample (control spinal cord WM) is annotated with an X. Bands are visible at approximately 16, 40, 60, 70 and 250 kDa.

Appendix A

Macro used for quantification Dab$^+$ pixels

```
path = getDirectory();
list = getFileList(path);
for(i = 0;i<list.length;i++){
open(path+list[i]);
imageTitle = getTitle();
run("Colour Deconvolution", "vectors = [User values] [r1] = 0.34028333 [g1] = 0.5633901 [b1] = 0.7528604 [r2] = 0.25282693 [g2] = 0.78388995 [b2] = 0.56709355 [r3] = 0.6048769 [g3] = 0.560661 [b3] = 0.56549376");
selectWindow(imageTitle+ "-(Colour_1)");
//run("Threshold...");
setThreshold(0,);
run("Measure");
}
```